Synthesis, Spectroscopic Characterization, and Structural Studies of Bis(μ-sulfido)bis[{*O,O*-dialkyl (alkylene) dithiophosphato}oxomolybdenum(V)] Complexes. Crystal Structures of Mo₂O₂S₂[S₂P(OEt)₂]₂, Mo₂O₂S₂[S₂P(OEt)₂]₂·2NC₅H₅, and Mo₂O₃[S₂P(OPh)₂]₄

John E. Drake,* Anil G. Mislankar, and Raju Ratnani[†]

Department of Chemistry and Biochemistry, University of Windsor, Windsor, Ontario, Canada N9B 3P4

Received April 26, 1995[⊗]

A series of new complexes, Mo₂O₂S₂[S₂P(OR)₂]₂ (where R = Et, *n*-Pr, *i*-Pr) and Mo₂O₂S₂[S₂POGO]₂ (where G = −CH₂CMe₂CH₂−, −CMe₂CMe₂−) have been prepared by the dropwise addition of an ethanolic solution of the ammonium or sodium salt of the appropriate *O,O*-dialkyl or -alkylene dithiophosphoric acid, or the acid itself, to a hot aqueous solution of molybdenum(V) pentachloride. The complexes were also formed by heating solutions of Mo₂O₃[S₂P(OR)₂]₄ or Mo₂O₃[S₂POGO]₄ species in glacial acetic acid. The Mo₂O₂S₂[S₂P(OR)₂]₂ and Mo₂O₂S₂[S₂POGO]₂ compounds were characterized by elemental analyses, ¹H, ¹³C, and ³¹P NMR, and infrared and Raman spectroscopy, as were the 1:2 adducts formed on reaction with pyridine. The crystal structures of Mo₂O₂S₂[S₂P(OEt₂)]₂, Mo₂O₂S₂[S₂P(OEt)₂]₂·2NC₅H₅, and Mo₂O₃[S₂P(OPh)₂]₄ were determined. Mo₂O₂S₂[S₂P-(OEt)₂]₂ (**1**) crystallizes in space group *C2/c*, No. 15, with cell parameters *a* = 15.644(3) Å, *b* = 8.339(2) Å, *c* = 18.269(4) Å, β = 103.70(2)°, *V* = 2315.4(8) Å³, *Z* = 4, *R* = 0.0439, and R_w = 0.0353. Mo₂O₂S₂[S₂P-(OEt)₂]₂·2NC₅H₅ (**6**) crystallizes in space group *P1̄*, No. 2, with the cell parameters *a* = 12.663(4) Å, *b* = 14.291-(5) Å, *c* = 9.349(3) Å, α = 100.04(3)°, β = 100.67(3)°, γ = 73.03(3)° *V* = 1557(1) Å³, *Z* = 2, *R* = 0.0593, and R_w = 0.0535. Mo₂O₃[S₂P(OPh)₂]₄ (**8**) crystallizes in space group *P2₁/n*, No. 14, with cell parameters *a* = 15.206-(2)Å, *b* = 10.655(3)Å, *c* = 19.406(3)Å, β = 111.67(1)°, *V* = 2921(1)Å³, *Z* = 2, *R* = 0.0518, R_w = 0.0425. The immediate environment about the molybdenum atoms in **1** is essentially square pyramidal if the Mo−Mo interaction is ignored. The vacant positions in the square pyramids are occupied by two pyridine molecules in **6**, resulting in an octahedral environment with very long Mo−N bonds. The terminal oxygen atoms in both **1** and **6** are in the *syn* conformation. In **8**, which also has a distorted octahedral environment about molybdenum, two of the dithiophosphate groups are bidentate as in **1** and **6**, but the two others have one normal Mo−S bond and one unusually long Mo−S bond.

Introduction

Oxomolybdenum complexes, with molybdenum in oxidation states IV, V, and VI, have been reported with 1,1-dithio ligands such as *N,N*-dialkyldithiocarbamates,[1−12] *O*-alkyl dithiocarbonates,[12−14] and *O,O*-dialkyl (alkylene) dithiophosphates.[7,12,15−19] Complexes containing the [Mo₂O₄]²⁺ unit are

only known for *N,N*-dialkyldithiocarbamates[20−23] and attempts to prepare similar complexes with *O*-alkyl dithiocarbonates resulted in the formation of the well-known [Mo₂O₃]⁴⁺ species.[14] Dithiocarbamate (dtc) complexes containing sulfur and/or oxygen bridging atoms such as Mo₂O₃S(dtc)₂,[21,24] Mo₂O₂S₂(dtc)₂,[8] Mo₂OS₃(dtc)₂,[21] and Mo₂S₄(dtc)₂,[23,25,26] have been reported but only [Mo₂O₂S₂]²⁺ and [Mo₂O₃S]²⁺ compounds have been reported, with *O*-alkyl dithiocarbonates[14] and *O,O*-dialkyl

(1) Bradbury, J. R.; Schultz, F. A. *Inorg. Chem.* **1986,** *25,* 4416.
(2) Devore, D. D. Maatta, E. A. *Inorg. Chem.* **1985,** *24,* 2846.
(3) Young, C. G.; Roberts, S. A.; Ortega, R. B.; Enemark, J. H. *J. Am. Chem. Soc.* **1987,** *109,* 2938.
(4) Chou, C. Y.; Devore, D. D.; Huckett S. C. Maatta, E. A. *Polyhedron* **1986,** *5,* 301.
(5) Barral, R.; Bocard, C.; Seree de Roch, I.; Sajus, L. *Tetrahedron Lett.* **1972,** *17,* 1693.
(6) Ricard, L.; Weiss, R. *Inorg. Nucl. Chem. Lett.* **1974,** *10,* 217.
(7) Chen, G. J. J.; McDonald, J. W.; Newton, W. E. *Inorg. Nucl. Chem. Lett.* **1976,** *15,* 2612.
(8) Moore, F. W.; Larson, M. L. *Inorg. Chem.* **1967,** *6,* 998.
(9) Kopwillen, A. *Acta Chem. Scand.* **1972,** *26,* 2941.
(10) Ricard, L.; Estienne, J.; Karagiannidis, P.; Toledano, P.; Mitchell A.; Weiss, R. *J. Coord. Chem.* **1974,** *3,* 277.
(11) Newton, W. E.; Bravard D. C.; McDonald, J. W. *Inorg. Nucl. Chem. Lett.* **1975,** *11,* 553.
(12) Jowitt, R. N.; Mitchell, P. C. H. *J. Chem. Soc. A* **1970,** 1702.
(13) Blake, A. B.; Cotton F. A.; Wood, J. S. *J. Am. Chem. Soc.* **1964,** *86,* 3024.
(14) Newton, W. E.; Corbin, J. L.; McDonald, J. W. *J. Chem. Soc., Dalton Trans.* **1974,** 1044.
(15) Chen, G. J. J.; McDonald, J. W.; Newton, W. E. *Inorg. Nucl. Chem. Lett.* **1976,** *12,* 697.
(16) Roberts, S. A.; Young, C. G.; Cleland, W. E.; Ortega R. B.; Enemark, J. H. *Inorg. Chem.* **1988,** *27,* 3044.
(17) Knox, J. R.; Prout, C. K. *Acta Crystallogr.* **1969,** *25B,* 2281.
(18) Jowitt, R. N.; Mitchell, P. C. H. *J. Chem. Soc. A,* **1969,** 2632.
(19) Edelblut, A. W.; Wentworth, R. A. D. *Inorg. Chem.* **1980,** *19,* 2006.
(20) Newton, W. E.; Corbin, J. L.; Bravard, D. C.; Searles J. E.; McDonald, J. W. *Inorg. Chem.* **1974,** *13,* 1100.
(21) Schultz, F. A.; Ott, V. R.; Rolison, D. S.; Bravard, D. C.; McDonald, J. W.; Newton, W. E. *Inorg. Chem.* **1978,** *17,* 1758.
(22) Ricard, L.; Martin, C.; Weist, R.; Weiss, R. *Inorg. Chem.* **1975,** *14,* 2300.
(23) Spivack, B.; Dori, Z; Steifel, E. I. *Inorg. Nucl. Chem. Lett.* **1975,** *11,* 501.
(24) Newton, W. E.; Chen, G. J. J.; McDonald, J. W. *J. Am. Chem. Soc.* **1976,** *98,* 5387.
(25) Sakurai, T.; Okabe, H.; Soyama, H. I. *Bull. Jpn. Pet. Inst.* **1971,** *13,* 243.
(26) Nagaraja, K. S.; Udupa, M. R. *Polyhedron* **1985,** *4,* 649.

dithiophosphates,[27,28] with the exception of the report of the crystal structure of $Mo_2O_2S_2[S_2P\{O(i\text{-}Pr)\}_2]_2$.[29]

The preparation of bis(μ-oxo)molybdenum(V) complexes with *O,O*-dialkyl (alkylene) dithiophosphates (dtp) was attempted, based on methodology established by earlier workers for the formation of $Mo_2O_4(dtc)_2$[20,21] and $Mo_2O_3(OAc)_2(dtc)_2$ species.[12] Although this method failed to produce $Mo_2O_4(dtp)_2$ complexes,[30] we discovered the first one-pot preparation of the arguably more interesting $Mo_2O_2S_2(dtp)_2$ species and report on the synthesis and characterization of bis(μ-sulfido)bis[{*O,O*-dialkyl (alkylene) dithiophosphato}oxomolybdenum(V)] complexes, $Mo_2O_2S_2[S_2P(OR)_2]_2$ (where R = Et, *n*-Pr, *i*-Pr) and $Mo_2O_2S_2[S_2POGO]_2$ (where G = $-CH_2CMe_2CH_2-$, $-CMe_2$-CMe_2-), and reactions with pyridine. X-ray crystal structures are reported for $Mo_2O_2S_2[S_2P(OEt)_2]_2$ (**1**), $Mo_2O_2S_2[S_2P$-$(OEt)_2]_2 \cdot 2NC_5H_5$ (**6**) and $Mo_2O_3[S_2P(OPh)_2]_4$ (**8**).

Experimental Section

Materials. $MoCl_5$ was obtained from Aldrich. Literature methods were used for the preparation of *O,O*-dialkyl,[31] *O,O*-diphenyl,[32] and *O,O*-alkylene[33] dithiophosphoric acids and for $Mo_2O_3[S_2P(OR)_2]_4$ and $Mo_2O_3[S_2POGO]_4$.[34] Sodium or ammonium salts of the dithiophosphoric acids were prepared by the reaction of the parent acids with an equimolar amount of sodium isopropoxide or ammonia in benzene.

Preparation of bis(μ-sulfido)bis[{*O,O*-diethyl, -dipropyl, and -diisopropyl dithiophosphato}oxomolybdenum(V)], $Mo_2O_2S_2[S_2P$-$(OEt)_2]_2$ (1), $Mo_2O_2S_2[S_2P\{O(n\text{-}Pr)\}_2]_2$ (2), and $Mo_2O_2S_2[S_2P\{O(i\text{-}Pr)\}_2]_2$ (3). Typically, an ethanolic solution (20 mL) of $NH_4S_2P(OEt)_2$ (1.20 g, 5.91 mmol) was added dropwise to a hot aqueous solution (20 mL) of $MoCl_5$ (1.54 g, 5.63 mmol) with constant stirring at approximately 60 °C. The purple solid that formed initially turned yellow as the mixture was maintained at 60 °C for a further 2 h. On cooling to room temperature, yellow crystals of bis(μ-sulfido)bis[{*O,O*-diethyl dithiophosphato}oxomolybdenum(V)] (**1**) were separated, washed with *n*-hexane, dried under vacuum, redissolved in a benzene/*n*-hexane (1:2) mixture, and recrystallized at -6 °C to give $Mo_2O_2S_2[S_2P(OEt)_2]_2$ (**1**): pale-yellow crystals, 0.84 g, yield 46%, mp 125–126 °C. Anal. Calcd for $C_8H_{20}O_6S_6P_2Mo_2$: Mo, 29.14; S, 29.21. Found: Mo, 28.46; S, 28.52. Molecular weight determined osmometrically in chloroform: 671.5; calcd 658.4. Similarly $Mo_2O_2S_2[S_2P\{O(n\text{-}Pr)\}_2]_2$ (**2**) was formed: yellow crystals, yield 35%, mp 150 °C. Anal. Calcd for $C_{12}H_{28}O_6S_6P_2Mo_2$: Mo, 26.85; S, 26.92. Found: Mo, 27.10; S, 26.47. $Mo_2O_2S_2[S_2P\{O(i\text{-}Pr)\}_2]_2$ (**3**) was also formed: yellow crystals, yield 45%, mp 125–126 °C. Anal. Calcd for $C_{12}H_{28}O_6S_6P_2Mo_2$: Mo, 26.85; S, 26.92. Found: Mo, 27.88; S, 27.30.

Preparation of Bis(μ-sulfido)bis[{*O,O*-2,2-dimethylpropylene and $-2,3$-dimethylbutylene dithiophosphato} oxomolybdenum(V)], $Mo_2O_2S_2[S_2POCH_2CMe_2CH_2O]_2$ (4) and $Mo_2O_2S_2[S_2POCMe_2$-$CMe_2O]_2$ (5). Typically, an ethanolic solution (20 mL) of NaS_2POCH_2-CMe_2CH_2O (1.00 g, 4.33 mmol) was added dropwise with constant stirring to a hot aqueous solution (20 mL) of $MoCl_5$ (1.14 g, 4.17 mmol) in a manner similar to that described above. The purple solid obtained initially, turned green as the mixture was held at 60 °C for a further 2 h. On cooling to room temperature, the precipitate of bis(μ-sulfido)-

bis[{*O,O*-2,2-dimethyl propylene dithiophosphato}oxomolybdenum(V)] was filtered off, washed with ethanol and dried under vacuum to give $Mo_2O_2S_2[S_2POCH_2CMe_2CH_2O]_2$ (**4**): green solid, 0.70 g, yield 49%, decpt >200 °C. Anal. Calcd for $C_{10}H_{20}O_6P_2S_6Mo_2$: Mo, 28.11; S, 28.19. Found: Mo, 28.94; S, 27.73. Similarly $Mo_2O_2S_2[S_2POCMe_2$-$CMe_2O]_2$ (**5**) was prepared: green solid, yield 57%, decpt >170 °C. Anal. Calcd for $C_{12}H_{24}O_6S_6P_2Mo_2$: Mo, 27.00; S, 27.07. Found: Mo, 26.64; S, 28.22. Neither **4** nor **5** are readily soluble in benzene or *n*-hexane, and attempts to form crystals from chloroform, dichloromethane, and various mixed solvents were not successful. The solids turned brown as they decomposed when attempts were made to record their melting points.

Alternative Preparations of $Mo_2O_2S_2[S_2P(OR)_2]_2$ and $Mo_2O_2S_2$-$[S_2POGO]_2$ Derivatives. Typically, an ethanolic solution (15 mL) of $HS_2P(OEt)_2$ (0.46 g, 2.47 mmol) was added dropwise to a hot aqueous solution of $MoCl_5$ (0.62 g, 2.27 mmol) with constant stirring. The initial purple solid changed to yellow as the mixture was heated for a further 2 h. On cooling to room temperature, yellow crystals formed which were washed with *n*-hexane and dried under vacuum to give $Mo_2O_2S_2[S_2P(OEt)_2]_2$ (**1**): 0.33 g, yield 44%, mp 125–126 °C. Anal. Calcd for $C_8H_{20}O_6S_6P_2Mo_2$: Mo, 29.14; S, 29.21; Found: Mo, 28.92; S, 28.74. Similarly from $HS_2POCH_2CMe_2CH_2O$ was formed $Mo_2O_2S_2$-$[S_2POCH_2CMe_2CH_2O]_2$ (**4**): green solid, 0.47 g, yield 47%, decpt >200 °C. Anal. Calcd for $C_{10}H_{20}O_6P_2S_6Mo_2$: Mo, 28.11; S, 28.19. Found: Mo, 28.54; S, 28.38.

Alternative Preparations of $Mo_2O_2S_2[S_2P(OEt)_2]_2$ (1) and $Mo_2O_2S_2$-$[S_2POCH_2CMe_2CH_2O]_2$ (4). Typically, an acetic acid solution (25 mL) of $Mo_2O_3[S_2P(OEt)_2]_4$ (1.34 g, 1.36 mmol) was heated on a steam bath until the color changed from red to yellow. The yellow crystals, which formed after the solution was kept for several days at room temperature, were washed with *n*-hexane and dried under vacuum to give $Mo_2O_2S_2[S_2P(OEt)_2]_2$ (**1**): 0.51 g, yield 46%, mp 125–126 °C. Anal. Calcd for $C_8H_{20}O_6S_6P_2Mo_2$: Mo, 29.14; S, 29.21; Found: Mo, 29.60; S, 28.73. Similarly from $Mo_2O_3[S_2POCH_2CMe_2CH_2O]_4$ was formed $Mo_2O_2S_2[S_2POCH_2CMe_2CH_2O]_2$ (**4**): green solid, 0.47 g, yield 47%, decpt >200 °C. Anal. Calcd for $C_{10}H_{20}O_6P_2S_6Mo_2$: Mo, 28.11; S, 28.19. Found: Mo, 28.54; S, 28.38.

Attempted Preparation of $Mo_2O_2S_2[S_2P(OPh)_2]_2$ from Mo_2O_3-$[S_2P(OPh)_2]_4$ (8). Attempts to prepare $Mo_2O_2S_2[S_2P(OPh)_2]_2$ by similarly heating $Mo_2O_3[S_2P(OPh)_2]_4$ in acetic acid were unsuccessful, the latter showing no signs of any solubility in the acetic acid. However X-ray quality crystals of $Mo_2O_3[S_2P(OPh)_2]_4$ were obtained on recrystallization from dichloromethane and a FAB mass spectrum obtained of the same material. These results are summarised as follows: peaks corresponding to clusters containing molybdenum are centered at *m/z* (relative intensities of highest peak in the cluster) 1084 ($Mo_2O_3L_3H^+$, 7%), 851 (most probably $Mo_2O_2S_2L_2H^+$ but indistinguishable from $Mo_2O_4SL_2H^+$ or $Mo_2O_6L_2H^+$, which are increasingly less probable, 16%), and 676 ($MoOL_2^+$, 100%) with a sharp peak clearly not part of a molybdenum cluster at *m/z* 563 (HL_2^+, 15%).

Preparation of Pyridine Adducts of $Mo_2O_2S_2[S_2P(OEt)_2]_2$ and $Mo_2O_2S_2[S_2PCH_2CMe_2CH_2O]_2$. Preparation of $Mo_2O_2S_2[S_2P$-$(OEt)_2]_2 \cdot 2NC_5H_5$ (6). Typically, a benzene solution (2 mL) of pyridine (0.099 g, 1.25 mmol) was added dropwise to a benzene/*n*-hexane (1:2) solution (15 mL) of $Mo_2O_2S_2[S_2P(OEt)_2]_2$ (0.324 g, 0.49 mmol). The solution was stirred for 15 min and then kept in the refrigerator overnight when bright yellow crystals were formed. The solvent was decanted and the crystals dried under vacuum to give $Mo_2O_2S_2[S_2P$-$(OEt)_2]_2 \cdot 2NC_5H_5$ (**6**): yellow crystals, 0.301 g, yield 71%, mp 82–83 °C. Anal. Calcd for $C_{18}H_{30}N_2O_6S_6P_2Mo_2$: Mo, 23.53; S, 15.72; Found: Mo, 22.90; S, 16.02.

Preparation of $Mo_2O_2S_2[S_2PCH_2CMe_2CH_2O]_2 \cdot 2NC_5H_5$ (7). Typically, a dichloromethane/*n*-hexane (1:1) solution (10 mL) of pyridine (0.089 g, 1.13 mmol) was added dropwise to a dichloromethane solution (15 mL) of $Mo_2O_2S_2[S_2PCH_2CMe_2CH_2O]_2$ (0.271 g, 0.40 mmol) and

(27) Black, A. L.; Dunster, R. W.; Sanders, J. V. *Wear* **1969**, *13*, 119.
(28) Drew, M. G. B.; Mitchell, P. C. H.; Read, A. R. *Acta Crystallogr.* **1981**, *37B*, 1758.
(29) Atovmyan, L. O.; Trachev, V. V.; Shchepinov, S. A. *Koord. Khim.* **1978**, *4*, 610.
(30) Ratnani, R. Doctoral Thesis, University of Rajasthan, Jaipur, India.
(31) Wasson, J. R.; Woltermann, G. M.; Stoklosa, H. J. *Top. Curr. Chem.* **1973**, *35*, 65.
(32) Fletcher, J. H.; Hamilton, I. H.; Hoegberg, E. I.; Sertl, B. J.; Cassaday. J. T. *J. Am. Chem. Soc.* **72**, 2461 (1950).
(33) Chauhan, H. P. S.; Bhasin, C. P.; Srivastava, G.; Mehrotra, R. C. *Phosphorus Sulfur* **1983**, *15*, 99.
(34) Ratnani, R.; Srivastava, G.; Mehrotra, R. C. *Inorg. Chim. Acta* **1989**, *161*, 253.

Table 1. Crystallographic Data for Mo$_2$O$_2$S$_2$[S$_2$P(OEt)$_2$]$_2$ (**1**), Mo$_2$O$_2$S$_2$[S$_2$P(OEt)$_2$]$_2$·2NC$_5$H$_5$ (**6**) and Mo$_2$O$_3$[S$_2$P(OPh)$_2$]$_4$ (**8**)

	1	**6**	**8**
chem formula	C$_8$H$_{20}$O$_6$S$_6$-P$_2$Mo$_2$	C$_{18}$H$_{30}$N$_2$O$_6$S$_6$-P$_2$Mo$_2$	C$_{24}$H$_{20}$O$_6$S$_6$-P$_2$Mo$_2$
a, Å	15.644(3)	12.663(4)	15.206(2)
b, Å	8.339(2)	14.291(5)	10.655(3)
c, Å	18.269(4)	9.349(3)	19.406(3)
α, deg	90.00	100.04(3)	90.00
β, deg	103.70(2)	100.67(3)	111.67(1)
γ, deg	90.00	73.03(3)	90.00
V, Å^3	2315.4(8)	1577(1)	2921(1)
space group	$C2/c$ (No. 15)	$P\bar{1}$ (No. 2)	$P2_1/n$ (No. 14)
fw	658.43	816.63	1365.09
Z	4	2	2
ρ_{calcd}, g cm^{-3}	1.89	1.72	1.55
μ, cm^{-1}	17.82	13.34	8.53
abs range	0.79−1.00	0.83−1.00	0.85−1.00
T, °C	23	23	23
λ, Å	0.710 69		
R^a	0.0439	0.0593	0.0544
$R_w{}^b$	0.0353	0.0535	0.0451
GoF	1.73	2.78	1.44

^{a} $R = \sum ||F_o| - |F_c||/\sum|F_o|$. ^{b} $R_w = [(\sum w(|F_o| - |F_c|)^2/\sum wF_o2)]^{1/2}$.

a yellow precipitate was formed immediately. The solution was stirred for a further 15 min before the precipitate was filtered, washed with *n*-hexane, and dried under vacuum to give Mo$_2$O$_2$S$_2$-[S$_2$PCH$_2$CMe$_2$CH$_2$O]$_2$·2NC$_5$H$_5$: yellow powder, 0.283 g, yield 85%, decpt > 200 °C. Anal. Calcd for C$_{20}$H$_{30}$N$_2$O$_6$S$_6$P$_2$Mo$_2$: Mo, 22.84; S, 15.26; Found: Mo, 23.25; S, 15.84.

Physical Measurements. All solvents were dried and distilled prior to use. Molybdenum was estimated by precipitation as molybdenum oxinate, MoO$_2$(C$_9$H$_6$ON)$_2$, and sulfur was estimated gravimetrically as barium sulfate (Messenger's method). The infrared spectra were recorded on a Nicolet 5DX FT spectrometer as CsI pellets and the far-infrared spectra on a Bomem IR Spectrometer between polyethylene films. The Raman spectra were recorded on a Ramanor U-1000 spectrometer using the 5145−Å exciting line of an argon ion laser with samples sealed in capillary tubes. The ^{1}H and ^{13}C NMR spectra were recorded on a Bruker 300 FT/NMR spectrometer in CDCl$_3$/CH$_2$Cl$_2$ using Me$_4$Si as internal standard. The ^{31}P NMR spectra were recorded on a Bruker 200 FT/NMR spectrometer in CDCl$_3$/CH$_2$Cl$_2$ using H$_3$-PO$_4$ as external standard. The melting points were determined on a Fisher-Johns apparatus.

X-ray Crystallographic Analysis. Yellow block crystals of Mo$_2$O$_2$S$_2$-[S$_2$P(OEt)$_2$]$_2$ (**1**) and Mo$_2$O$_2$S$_2$[S$_2$P(OEt)$_2$]$_2$·2NC$_5$H$_5$ (**6**) and a purple block crystal of Mo$_2$O$_3$[S$_2$P(OPh)$_2$]$_4$ (**8**) were sealed in thin-walled glass capillaries and mounted on a Rigaku AFC6S diffractometer, with graphite-monochromated Mo Kα radiation.

Cell constants and an orientation matrix for data collection, obtained from a least-squares refinement using the setting angles of 24 (for **1**), 15 (for **6**) and 20 (for **8**) carefully centered reflections in the range 20.05 < 2θ < 27.37° (for **1**), 7.78 < 2θ < 12.15° (for **6**), and 12.7< 2θ < 18.3° (for **8**) corresponded to monoclinic (**1** and **8**) and triclinic (**6**) cells whose dimensions are given in Table 1. For **1** and **8** the systematic absences (h0l, h+l ≠ 2n; 0k0, k ≠ 2n) and (hkl, h+k ≠ 2n; h0l, l ≠ 2n), respectively, are observed. Based on packing considerations, statistical analyses of intensity distributions, and the successful solution and refinement of the structures, the space groups were determined to be $C2/c$ (No. 15) for **1**, $P\bar{1}$ (No. 2) for **6**, and $P2_1/n$ (No. 14) for **8**.

The data were collected at a temperature of 23 ± 1 °C using the ω−2θ scan technique to a maximum 2θ value of 50.0°. The ω scans of several intense reflections, made prior to data collection, had an average width at half-height of 0.27° for **1**, 0.29 for **6**, and 0.32° for **8** with a takeoff angle of 6.0°. Scans of (1.68 + 0.30 tan θ)° for **1**, (1.63 + 0.30 tan θ)° for **6**, and (1.00 + 0.30 tan θ)° for **8** were made at speeds of 8.0 (**1** and **8**) and 16 (**6**)deg/min (in ω). The weak reflections (*I* < 10.0σ(*I*)) were rescanned (maximum of two rescans), and the counts were accumulated to assure good counting statistics. Stationary background counts were recorded on each side of the

reflection. The ratio of peak counting time to background counting time was 2:1. The diameter of the incident beam collimator was 1.0 mm, and the crystal to detector distance was 250.0 mm.

Of the 2289 (for **1**), 5807 (for **6**) or 5668 (for **8**) reflections which were collected, 2202 (for **1**), 5532 (for **6**), or 5452 (for **8**) were unique (R_{int} = 0.097, 0.037 or 0.107). The intensities of three representative reflections which were measured after every 150 reflections remained constant throughout data collection, indicating crystal and electronic stability (no decay correction was applied).

The linear absorption coefficient for Mo Kα is 17.82 cm^{-1} (for **1**), 13.34 cm^{-1} (for **6**), and 8.53 cm^{-1} (for **8**). An empirical absorption correction, based on azimuthal scans of several reflections, was applied which resulted in transmission factors ranging from 0.79 to 1.00 (for **1**), 0.83 to 1.00 (for **6**), and 0.85 to 1.00 (for **8**). The data were corrected for Lorentz and polarization effects.

The structures were solved by direct methods.[35] The non-hydrogen atoms were refined anisotropically and the hydrogen atoms were included in their idealised positions with C−H set at 0.95 Å and with isotropic thermal parameters set at 1.2 times that of the carbon atom to which they were attached. The phenyl rings in **8** were constrained to a regular hexagon with C−C bond distances of 1.395 Å and C−C−C angles of 120.0°. One of the OEt groups in **2** is disordered and was modelled to obtain convergence. The final cycle of full-matrix least-squares refinement[36] was based on 754 (for **1**), 3744 (for **6**), and 1456 (for **8**) observed reflections (*I* > 3.00σ(*I*)) and 97 (for **1**), 325 (for **6**) and 143 (for **8**) variable parameters and converged (largest parameter shift was 0.001 times its esd) with unweighted and weighted agreement factors of $R = \sum ||F_o| - |F_c||/\sum|F_o|$ = 0.0439 (for **1**), 0.0593 (for **6**), and 0.0544 (for **8**) and $R_w = [(\sum w(|F_o| - |F_c|)^2/\sum wF_o2)]^{1/2}$ = 0.0353 (for **1**), 0.0535 (for **6**) and 0.0451 (for **8**).

The standard deviations of an observation of unit weight[37] were 1.38, 2.78, and 1.44 (for **1**, **6** and **8**), respectively. The weighting scheme was based on counting statistics and included a factor (p = 0.005 for **1**, 0.006 for **6** and 0.002 for **8**) to downweight the intense reflections. Plots of $\sum w(|F_o| - |F_c|)^2$ vs $|F_o|$, reflection order in data collection, sin θ/λ, and various classes of indices showed no unusual trends. The maximum and minimum peaks on the final difference Fourier map corresponded to +0.45 and −0.40 e/Å^3 (for **1**) +1.42 and −0.98 (for **6**), and +0.79 and −0.57 e/Å^3 (for **8**).

Neutral-atom scattering factors were taken from Cromer and Waber.[38] Anomalous dispersion effects were included in F_c;[39] the values for Δf' and Δf'' were those of Cromer.[40] All calculations were performed using the TEXSAN[41] crystallographic software package of the Molecular Structure Corp.

The final atomic coordinates and equivalent isotropic thermal parameters for the non-hydrogen atoms are given in Tables 2−4, important distances and bond angles for **1** and **6** in Tables 5 and 6 and for **8** in Table 7, and ORTEP diagrams in Figures 1−3. Additional crystallographic data are available as Supporting Information.

Results and Discussion

The dropwise addition of an ethanolic solution of the ammonium or sodium salt of the appropriate dialkyl or alkylene dithiophosphoric acid to a hot, stirred, aqueous solution of molybdenum(V) pentachloride results in the initial formation

(35) Sheldrick, G. M. *Crystallographic Computing 3*; Sheldrick, G. M.; Kruger, C.; Goddard, R., Eds.; Oxford University Press: Oxford, England, 1985; p 175.

(36) Least-squares: Function minimized: $\sum w(|F_o| - |F_c|)^2$, where w = $4F_o^2(F_o^2)$, $\sigma^2(F_o^2)$ = [S^2($C + R^2B$) + (pF_o2)^2]/(Lp)^2, S = scan rate, C = total integrated peak count, R = ratio of scan time to background counting time, Lp = Lorentz-polarization factor, and p = p factor.

(37) Standard deviation of an observation of unit weight: [$\sum w(|F_o| - |F_c|)^2$/$N_o - N_v$]$^{1/2}$, where N_o = number of observations and N_v = number of variables.

(38) Cromer, D. T.; Waber, J. T. *International Tables for X-ray Crystallography*; The Kynoch Press: Birmingham, England, 1974; Vol. IV, Table 2.2 A.

(39) Ibers, J. A.; Hamilton, W. C. *Acta Crystallogr.* **1964**, *17*, 781.

(40) Cromer, D. T. *International Tables for X-ray Crystallography*; The Kynoch Press: Birmingham, England, 1974; Vol. IV, Table 2.3.1.

(41) *TEXSAN-TEXRAY Structure Analysis Package*; Molecular Structure Corp.: Woodlands, TX, 1985.
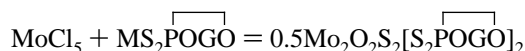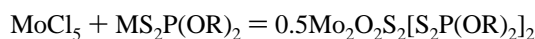
Table 2. Final Fractional Coordinates and B(eq) Values for Non-Hydrogen Atoms of $Mo_2O_2S_2[S_2P(OEt)_2]_2$ (**1**) with Standard Deviations in Parentheses

atom	x	y	z	B(eq),Å^2
Mo(1)	0.43596(9)	0.2497(2)	0.29315(8)	4.12(5)
S(1)	0.4162(3)	0.2963(5)	0.1649(2)	5.1(2)
S(2)	0.4342(3)	0.3439(5)	0.4231(2)	5.9(3)
S(3)	0.3006(3)	0.4128(6)	0.2689(2)	5.7(2)
P(1)	0.3144(3)	0.4350(6)	0.3805(2)	5.5(3)
O(1)	0.4131(7)	0.057(1)	0.3016(6)	6.6(6)
O(2)	0.3047(7)	0.607(1)	0.4090(7)	6.7(7)
O(3)	0.2383(9)	0.351(2)	0.4114(7)	10.1(9)
C(1)	0.361(1)	0.732(3)	0.402(1)	8.1(5)
C(2)	0.349(1)	0.868(2)	0.451(1)	8.0(5)
C(3a)	0.178(2)	0.230(4)	0.385(2)	7.8(7)
C(3b)	0.141(5)	0.354(9)	0.380(4)	8(1)
C(4a)	0.099(2)	0.275(6)	0.345(2)	8(1)
C(4b)	0.094(3)	0.27(1)	0.385(3)	8(1)

Table 3. Final Fractional Coordinates and B(eq) Values for Non-Hydrogen Atoms of $Mo_2O_2S_2[S_2P(OEt)_2]_2 \cdot 2NC_5H_5$ (**6**) with Standard Deviations in Parentheses

atom	x	y	z	B(eq),Å^2
Mo(1)	0.04123(7)	0.66330(6)	0.25495(8)	2.63(4)
Mo(2)	−0.14794(6)	0.81991(6)	0.31081(8)	2.52(4)
S(1)	0.0308(2)	0.8318(2)	0.3039(2)	2.8(1)
S(2)	−0.1181(2)	0.6540(2)	0.3382(2)	3.2(1)
S(3)	0.2483(2)	0.6345(2)	0.2386(3)	4.0(1)
S(4)	0.1178(2)	0.4796(2)	0.2750(3)	4.0(1)
S(5)	−0.2003(2)	1.0068(2)	0.3757(3)	3.5(1)
S(6)	−0.3368(2)	0.8534(2)	0.3998(3)	3.7(1)
P(1)	0.2658(3)	0.4960(2)	0.2677(3)	4.8(2)
P(2)	−0.3362(2)	0.9941(2)	0.4432(3)	3.3(1)
O(1)	0.0058(5)	0.6475(5)	0.0723(6)	4.0(4)
O(2)	−0.2081(5)	0.8246(5)	0.1351(6)	3.7(3)
O(3)	0.3525(7)	0.4757(7)	0.420(1)	8.4(6)
O(4)	0.3365(8)	0.4113(7)	0.168(1)	9.2(7)
O(5)	−0.4452(5)	1.0670(5)	0.3730(7)	4.6(4)
O(6)	−0.3400(6)	1.0291(6)	0.6113(7)	5.2(5)
N(1)	0.1285(6)	0.6639(5)	0.5259(7)	3.0(4)
N(2)	−0.0946(6)	0.8380(5)	0.5884(7)	2.8(4)
C(1)	0.369(1)	0.398(1)	0.495(2)	11(1)
C(2)	0.465(2)	0.362(2)	0.554(3)	17(2)
C(3)	0.295(1)	0.393(1)	0.019(1)	10(1)
C(4)	0.391(2)	0.352(2)	−0.059(2)	13(2)
C(5)	−0.477(1)	1.058(1)	0.216(1)	6.4(8)
C(6)	−0.577(1)	1.133(1)	0.177(2)	12(1)
C(7)	−0.318(1)	1.112(1)	0.682(2)	7(1)
C(8)	−0.305(1)	1.121(1)	0.841(1)	9(1)
C(9)	0.2043(9)	0.7143(8)	0.584(1)	4.0(6)
C(10)	0.255(1)	0.7149(9)	0.729(1)	5.5(7)
C(11)	0.228(1)	0.659(1)	0.816(1)	5.6(7)
C(12)	0.152(1)	0.6083(9)	0.759(1)	5.2(7)
C(13)	0.1064(8)	0.6111(8)	0.615(1)	3.8(6)
C(14)	−0.0336(8)	0.8963(7)	0.657(1)	3.5(5)
C(15)	−0.004(1)	0.9089(9)	0.808(1)	5.4(7)
C(16)	−0.042(1)	0.8563(8)	0.893(1)	4.5(6)
C(17)	−0.106(1)	0.7976(8)	0.820(1)	4.6(6)
C(18)	−0.1299(8)	0.7890(7)	0.671(1)	3.5(5)

Table 4. Final Fractional Coordinates and B(eq) Values for Non-Hydrogen Atoms of $Mo_2O_3[S_2P(OPh)_2]_4$ (**8**) with Standard Deviations in Parentheses

atom	x	y	z	B(eq),Å^2
Mo(1)	0.1260(1)	0.0416(1)	0..52193(8)	2.56(6)
S(1)	0.0765(3)	0.2420(5)	0.4563(3)	4.2(2)
S(2)	0.2800(3)	0.1056(4)	0.5073(3)	3.6(2)
S(3)	0.1804(3)	−0.1817(4)	0.5439(2)	3.6(2)
S(4)	0.0896(3)	−0.0579(4)	0.3787(2)	3.7(2)
P(1)	0.2092(3)	0.2585(5)	0.4598(3)	3.3(2)
P(2)	0.1299(3)	−0.2135(4)	0.4342(2)	3.0(2)
O(1)	0	0	$^1/_2$	3.9(8)
O(2)	0.1637(7)	0.074(1)	0.6119(5)	3.8(5)
O(3)	0.2590(8)	0.384(1)	0.4963(6)	4.2(6)
O(4)	0.2026(7)	0.280(1)	0.3778(6)	4.0(6)
O(5)	0.0505(7)	−0.317(1)	0.4202(5)	3.6(5)
O(6)	0.2041(7)	−0.292(1)	0.4111(6)	3.7(5)
C(1)	0.282(1)	0.413(1)	0.5698(5)	6.9
C(2)	0.2187(7)	0.481(1)	0.5925(7)	6.9
C(3)	0.2428(9)	0.511(1)	0.6672(9)	6.9
C(4)	0.330(1)	0.473(1)	0.7192(5)	6.9
C(5)	0.3927(7)	0.405(1)	0.6966(7)	6.9
C(6)	0.369(1)	0.375(1)	0.6219(9)	6.9
C(7)	0.2841(6)	0.301(1)	0.3628(6)	5.6
C(8)	0.3172(8)	0.423(1)	0.3618(6)	5.6
C(9)	0.3967(9)	0.4438(9)	0.3438(6)	5.6
C(10)	0.4432(6)	0.342(1)	0.3268(6)	5.6
C(11)	0.4101(8)	0.221(1)	0.3277(6)	5.6
C(12)	0.3305(9)	0.2000(9)	0.3457(6)	5.6
C(13)	0.0015(7)	−0.366(1)	0.3510(5)	4.6
C(14)	−0.0759(8)	−0.3030(8)	0.3006(7)	4.6
C(15)	−0.1277(6)	−0.357(1)	0.2322(6)	4.6
C(16)	−0.1019(7)	−0.475(1)	0.2141(5)	4.6
C(17)	−0.0245(8)	−0.5381(8)	0.2645(6)	4.6
C(18)	0.0272(6)	−0.484(1)	0.3330(5)	4.6
C(19)	0.2870(7)	−0.242(1)	0.4103(8)	5.1
C(20)	0.371(1)	−0.244(1)	0.4729(6)	5.1
C(21)	0.4529(7)	−0.191(1)	0.4695(6)	5.1
C(22)	0.4519(7)	−0.137(1)	0.4037(7)	5.1
C(23)	0.368(1)	−0.136(1)	0.3412(5)	5.1
C(24)	0.2859(7)	−0.188(1)	0.3445(6)	5.1

These results are surprising because earlier workers using dithiocarbamate salts,[20,21] and dithiophosphinic acid[21] had established a route to bis(μ-oxo)molybdenum(V) complexes using similar experimental conditions.

$$MoCl_5 + NaS_2CNR_2 = 0.5Mo_2O_4[S_2CNR_2]_2$$
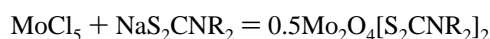
(R = Me, Et; NR$_2$ = 1-piperidine, 4-morpholine)

$$MoCl_5 + HS_2P(i\text{-}Pr)_2 = 0.5Mo_2O_4[S_2P(i\text{-}Pr)_2]_2$$
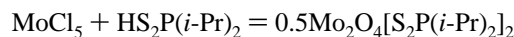
The $Mo_2O_2S_2[S_2P(OR)_2]_2$ and $Mo_2O_2S_2[S_2POGO]_2$ derivatives are obtained in yields ranging from 35% to 57% as yellow crystals and green solids, respectively. The acyclic derivatives are soluble in most common organic solvents, in contrast to the cyclic analogues, which are only found to be soluble in CH_2Cl_2 and $CHCl_3$, and only sparingly so in the latter case.

A yellow crystalline complex, $Mo_2O_3(OAc)_2(S_2CNEt_2)_2$, was obtained on heating $Mo_2O_3(S_2CNEt_2)_4$ in glacial acetic acid.[12] By contrast, when $Mo_2O_3[S_2P(OEt)_2]_4$ and $Mo_2O_3[\overline{S_2POCH_2CMe_2CH_2O}]_4$ are heated in glacial acetic acid, the bis(μ-sulfido) compounds, $Mo_2O_2S_2[S_2P(OEt)_2]_2$ and $Mo_2O_2S_2[\overline{S_2POCH_2CMe_2CH_2O}]_2$ are formed, providing another new, if unexpected, preparative route. The rearrangement, which apparently requires two sulfur atoms from displaced dithiophosphate ligands to replace the oxygen atom of the Mo−O−Mo bridge, does not take place with $Mo_2O_3[S_2P(OPh)_2]_4$. However, the mass

of a purple solid which changes color as the mixture is refluxed for 2 h. On cooling to −6 °C, a variety of bis(μ-sulfido)bis-[{O,O-dialkyl (alkylene) dithiophosphato}oxomolybdenum(V)] complexes, $Mo_2O_2S_2(dtp)_2$, are obtained in a one-pot conversion from $MoCl_5$.

$$MoCl_5 + MS_2P(OR)_2 = 0.5Mo_2O_2S_2[S_2P(OR)_2]_2$$

$$MoCl_5 + MS_2\overline{POGO} = 0.5Mo_2O_2S_2[S_2\overline{POGO}]_2$$

(M$^+$ = Na$^+$, NH$_4^+$, H$^+$; R = Et, n-Pr, i-Pr;
G = −CH$_2$CMe$_2$CH$_2$−, −CMe$_2$CMe$_2$−)

Table 5. Important Interatomic Distances (Å) for Mo$_2$O$_2$S$_2$[S$_2$P(OEt)$_2$]$_2$ (**1**) and Mo$_2$O$_2$S$_2$[S$_2$P(OEt)$_2$]$_2$·2NC$_5$H$_5$ (**6**)[a,b]

Mo$_2$O$_2$S$_2$[S$_2$P(OEt)$_2$]$_2$ (**1**)		Mo$_2$O$_2$S$_2$[S$_2$P(OEt)$_2$]$_2$·2NC$_5$H$_5$ (**6**)			
Mo(1)−Mo(1)′	2.828(3)	Mo(1)−Mo(2)	2.819(1)		
Mo(1)−S(1)	2.322(5)	Mo(1)−S(1)	2.341(3)	Mo(2)−S(1)	2.332(2)
Mo(1)−S(1)′	2.291(4)	Mo(1)−S(2)	2.338(3)	Mo(2)−S(2)	2.342(3)
Mo(1)−S(2)	2.508(5)	Mo(1)−S(3)	2.562(3)	Mo(2)−S(5)	2.548(3)
Mo(1)−S(3)	2.466(4)	Mo(1)−S(4)	2.547(3)	Mo(2)−S(6)	2.563(3)
Mo(1)−O(1)	1.66(1)	Mo(1)−O(1)	1.676(5)	Mo(2)−O(2)	1.681(5)
		Mo(1)−N(1)	2.569(7)	Mo(2)−N(2)	2.545(7)
S(2)−P(1)	2.001(6)	S(3)−P(1)	1.988(4)	S(5)−P(2)	2.004(3)
S(3)−P(1)	2.007(7)	S(4)−P(1)	1.970(4)	S(6)−P(2)	1.983(4)
P(1)−O(3)	1.64(1)	P(1)−O(3)	1.64(1)	P(2)−O(5)	1.576(7)
P(1)−O(4)	1.557(9)	P(1)−O(4)	1.557(9)	P(2)−O(6)	1.569(7)
O(2)−C(1)	1.39(2)	O(3)−C(1)	1.35(2)	O(5)−C(5)	1.44(1)
O(3)−C(3a)	1.39(3)	O(4)−C(3)	1.40(1)	O(6)−C(7)	1.33(1)
O(3)−C(3b)	1.50(7)				
C(1)−C(2)	1.49(2)	C(1)−C(2)	1.24(2)	C(5)−C(6)	1.43(2)
C(3a)−C(4a)	1.34(4)	C(3)−C(4)	1.45(2)	C(7)−C(8)	1.45(2)
C(3b)−C(4b)	1.04(9)				

[a] Symmetry equivalent position (1 − x, y, $^1/_2$ − z) is denoted by prime. [b] Numbers in parentheses refer to standard deviations in least significant digits.

Table 6. Important Bond Angles (deg) for Mo$_2$O$_2$S$_2$[S$_2$P(OEt)$_2$]$_2$ (**1**) and Mo$_2$O$_2$S$_2$[S$_2$P(OEt)$_2$]$_2$·2NC$_5$H$_5$ (**6**)[a,b]

Mo$_2$O$_2$S$_2$[S$_2$P(OEt)$_2$]$_2$ (**1**)		Mo$_2$O$_2$S$_2$[S$_2$P(OEt)$_2$]$_2$·2NC$_5$H$_5$ (**6**) Ph$_3$Ge[S$_2$POCH$_2$CMe$_2$CH$_2$O], 2			
Mo(1)′−Mo(1)−S(1)	51.7(1)	Mo(2)−Mo(1)−S(1)	52.76(6)	Mo(1)−Mo(2)−S(1)	53.04(6)
Mo(1)′−Mo(1)−S(1)′	52.7(1)	Mo(2)−Mo(1)−S(2)	53.01(6)	Mo(1)−Mo(2)−S(2)	52.91(6)
Mo(1)′−Mo(1)−S(2)	134.1(1)	Mo(2)−Mo(1)−S(3)	139.67(7)	Mo(1)−Mo(2)−S(5)	139.18(6)
Mo(1)′−Mo(1)−S(3)	126.2(1)	Mo(2)−Mo(1)−S(4)	139.72(7)	Mo(1)−Mo(2)−S(6)	140.43(7)
Mo(1)′−Mo(1)−O(1)	104.4(4)	Mo(2)−Mo(1)−O(1)	95.9(2)	Mo(1)−Mo(2)−O(1)	96.7(2)
		Mo(2)−Mo(1)−N(1)	94.5(2)	Mo(1)−Mo(2)−N(2)	95.0(2)
S(1)−Mo(1)−S(1)′	101.1(1)	S(1)−Mo(1)−S(2)	103.06(8)	S(1)−Mo(2)−S(2)	103.23(9)
S(1)−Mo(1)−S(2)	151.0(2)	S(1)−Mo(1)−S(3)	86.92(8)	S(1)−Mo(2)−S(5)	86.17(8)
S(1)−Mo(1)−S(3)	79.8(2)	S(1)−Mo(1)−S(4)	158.04(9)	S(1)−Mo(2)−S(6)	159.10(9)
S(1)−Mo(1)−O(1)	106.0(4)	S(1)−Mo(1)−O(1)	102.4(2)	S(1)−Mo(2)−O(2)	102.8(2)
S(1)′−Mo(1)−S(2)	82.4(2)	S(2)−Mo(1)−S(3)	159.09(8)	S(2)−Mo(2)−S(5)	158.59(8)
S(1)′−Mo(1)−S(3)	136.2(2)	S(2)−Mo(1)−S(4)	86.76(9)	S(2)−Mo(2)−S(6)	87.53(8)
S(1)′−Mo(1)−O(1)	110.8(4)	S(2)−Mo(1)−O(1)	101.2(2)	S(2)−Mo(2)−O(2)	102.7(2)
S(2)−Mo(1)−S(3)	78.2(1)	S(3)−Mo(1)−S(4)	78.06(9)	S(5)−Mo(2)−S(6)	78.12(8)
S(2)−Mo(1)−O(1)	99.4(4)	S(3)−Mo(1)−O(1)	93.4(2)	S(5)−Mo(2)−O(2)	93.7(2)
S(3)−Mo(1)−O(1)	110.8(4)	S(4)−Mo(1)−O(1)	94.5(2)	S(6)−Mo(2)−O(2)	92.0(2)
		N(1)−Mo(1)−O(1)	169.9(3)	N(2)−Mo(2)−O(2)	168.2(3)
Mo(1)−S(1)−Mo(1)′	75.6(1)	Mo(1)−S(1)−Mo(2)	74.20(7)		
Mo(1)−S(1)′−Mo(1)′	75.6(1)	Mo(1)−S(2)−Mo(2)	74.08(7)		
Mo(1)−S(2)−P(1)	88.2(2)	Mo(1)−S(3)−P(1)	86.1(1)	Mo(2)−S(5)−P(2)	87.0(1)
Mo(1)−S(3)−P(1)	89.3(2)	Mo(1)−S(4)−P(1)	86.9(1)	Mo(2)−S(6)−P(2)	87.0(1)
S(2)−P(1)−S(3)	103.1(3)	S(3)−P(1)−S(4)	108.8(2)	S(5)−P(2)−S(6)	107.7(2)
S(2)−P(1)−O(2)	112.3(5)	S(3)−P(1)−O(3)	106.8(4)	S(5)−P(2)−O(5)	111.1(3)
S(2)−P(1)−O(3)	113.8(6)	S(3)−P(1)−O(4)	118.4(4)	S(5)−P(2)−O(6)	113.2(3)
S(3)−P(1)−O(2)	115.6(6)	S(4)−P(1)−O(3)	113.1(4)	S(6)−P(2)−O(5)	114.0(3)
S(3)−P(1)−O(3)	114.2(6)	S(4)−P(1)−O(4)	113.4(4)	S(6)−P(2)−O(6)	109.4(3)
O(2)−P(1)−O(3)	98.5(8)	O(3)−P(1)−O(4)	95.7(6)	O(5)−P(2)−O(6)	101.5(4)
P(1)−O(2)−C(1)	123(1)	P(1)−O(3)−C(1)	125(1)	P(2)−O(5)−C(5)	120.2(7)
P(1)−O(3)−C(3b)	129(3)	P(1)−O(4)−C(3)	120(1)	P(2)−O(6)−C(7)	124.7(8)
O(2)−C(1)−C(2)	110(1)	O(3)−C(1)−C(2)	118(2)	O(5)−C(5)−C(6)	111(1)
O(3)−C(3a)−C(4a)	117(3)	O(4)−C(3)−C(4)	107(1)	O(6)−C(7)−C(8)	116(1)
		N(1)−C(9)−C(10)	123.4(9)	N(2)−C(14)−C(15)	123.3(8)
		C(9)−C(10)−C(11)	118(1)	C(14)−C(15)−C(16)	118.6(9)
		C(10)−C(11)−C(12)	119(1)	C(15)−C(16)−C(17)	117.2(9)
		C(11)−C(12)−C(13)	119.3(9)	C(16)−C(17)−C(18)	120.2(9)
		N(1)−C(13)−C(12)	124.4(9)	N(2)−C(18)−C(17)	123.5(9)

[a] Symmetry equivalent position (1 − x, y, $^1/_2$ − z) is denoted by prime. [b] Numbers in parentheses refer to standard deviations in least significant digits.

spectrum of Mo$_2$O$_3$[S$_2$P(OPh)$_2$]$_4$ has three sets of peaks in the fragmentation pattern that are associated with clusters containing one or two molybdenum atoms. The most prominent of these corresponds to MoO[S$_2$P(OPh)$_2$]$_2$$^+$, which is expected for fission of the Mo−O−Mo bridge. The fragment, Mo$_2$O$_3$[S$_2$P-(OPh)$_2$]$_3$H$^+$, arises from the loss of one ligand and Mo$_2$O$_2$S$_2$-[S$_2$P(OPh)$_2$]$_2$H$^+$ is consistent with the replacement of the bridging oxygen by two sulfur atoms along with the loss of two ligands.

Molecular Structures of Mo$_2$O$_2$S$_2$[S$_2$P(OEt)$_2$]$_2$ (1) and Mo$_2$O$_2$S$_2$[S$_2$P(OEt)$_2$]$_2$·2NC$_5$H$_5$ (6). For comparison, the bond lengths for **1** and **6** are given together in Table 5 and the bond angles in Table 6. Bis(μ-sulfido)bis[{O,O-diethyl dithio-phosphato}oxomolybdenum(V)] (**1**) crystallizes in the space group *C2/c* and its 1:2 pyridine adduct (**6**) in the space group *P*1̄. The structure of only one other analogous dithiophosphate has been reported, namely Mo$_2$O$_2$(μ-S)$_2$[S$_2${O(i-Pr)}$_2$]$_2$,[29] which crystallizes in the space group *Pbca*. The molecule in which

Table 7. Important Interatomic Distances (Å) and Bond Angles for Mo$_2$O$_3$[S$_2$P(OPh)$_2$]$_4$ (**8**)^{a,b}

Mo(1)−O(1)	1.8567(5)	Mo(1)−O(2)	1.66(1)
Mo(1)−S(1)	2.458(5)	Mo(1)−S(3)	2.503(5)
Mo(1)−S(2)	2.554(5)	Mo(1)−S(4)	2.831(4)
S(1)−P(1)	2.001(7)	S(3)−P(2)	2.007(6)
S(2)−P(2)	1.983(6)	S(4)−P(2)	1.949(6)
P(1)−O(3)	1.57(1)	P(2)−O(5)	1.58(1)
P(1)−O(4)	1.58(1)	P(2)−O(6)	1.60(1)
O(3)− C(1)	1.37(2)	O(5)−C(13)	1.38(1)
O(4)−C(7)	1.39(2)	O(6)−C(19)	1.37(2)
O(1)−Mo(1)−O(2)	102.5(4)	Mo(1)−O(1)−Mo(1)′	180.00
O(1)−Mo(1)−S(1)	89.8(1)	O(1)−Mo(1)−S(3)	93.5(1)
O(1)−Mo(1)−S(2)	161.7(1)	O(1)−Mo(1)−S(4)	82.8(1)
O(2)−Mo(1)−S(1)	106.5(4)	O(2)−Mo(1)−S(3)	93.1(4)
O(2)−Mo(1)−S(2)	95.0(4)	O(2)−Mo(1)−S(4)	167.5(4)
S(1)−Mo(1)−S(2)	80.1(2)	S(3)−Mo(1)−S(4)	75.2(1)
S(1)−Mo(1)−S(4)	84.6(2)	S(3)−Mo(1)−S(1)	158.9(2)
S(2)−Mo(1)−S(4)	81.1(1)	S(3)−Mo(1)−S(2)	90.8(2)
P(1)−S(1)−Mo(1)	86.9(2)	P(2)−S(3)−Mo(1)	90.4(2)
P(1)−S(2)−Mo(1)	84.7(2)	P(2)−S(4)−Mo(1)	82.4(2)
O(3)−P(1)−O(4)	99.8(7)	O(5)−P(2)−O(6)	99.1(6)
O(3)−P(1)−S(1)	113.7(6)	O(5)−P(2)−S(3)	105.7(5)
O(3)−P(1)−S(1)	113.8(4)	O(5)−P(2)−S(4)	115.7(4)
O(4)−P(1)−S(1)	107.0(4)	O(6)−P(2)−S(3)	110.7(4)
O(4)−P(1)−S(2)	114.2(5)	O(6)−P(2)−S(4)	113.7(5)
S(1)−P(1)−S(2)	108.2(3)	S(3)−P(2)−S(4)	111.2(3)
P(1)−O(3)−C(1)	123(1)	P(2)−O(5)−C(13)	122.6(9)
P(1)−O(4)−C(7)	120.4(7)	P(2)−O(6)−C(19)	123.0(9)

^{a} Symmetry equivalent position (−x, −y, 1 − z) is denoted by a prime. ^{b} Numbers in parentheses refer to standard deviations in least significant digits.
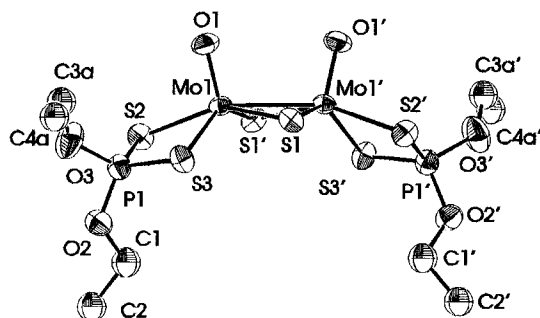
Figure 1. ORTEP plot of the molecule Mo$_2$O$_2$S$_2$[S$_2$P(OEt)$_2$]$_2$ (**1**). The atoms are drawn with 30% probability ellipsoids. Hydrogen atoms are omitted for clarity, as are the disordered atoms of the ethyl group, C(3b) and C(4b).
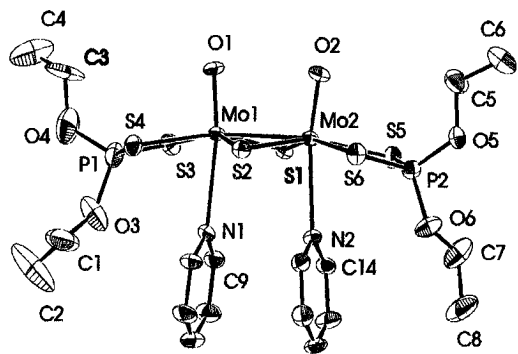
Figure 2. ORTEP plot of the molecule Mo$_2$O$_2$S$_2$[S$_2$P(OEt)$_2$]$_2$·2NC$_5$H$_5$ (**6**). The atoms are drawn with 30% probability ellipsoids. Hydrogen atoms are omitted for clarity.

one of the bridging sulfur atoms is replaced by one oxygen atom, namely Mo$_2$(μ-O,S)[S$_2${O(*i*-Pr)}$_2$]$_2$,[28] also crystallizes as *Pbca* and structures of its adducts with nitrogen donors have been reported.[42,43] The ORTEP diagram of Mo$_2$O$_2$(μ-S)$_2$[S$_2$P(OEt)$_2$]$_2$ (**1**) (Figure 1), which has been drawn with the second positions
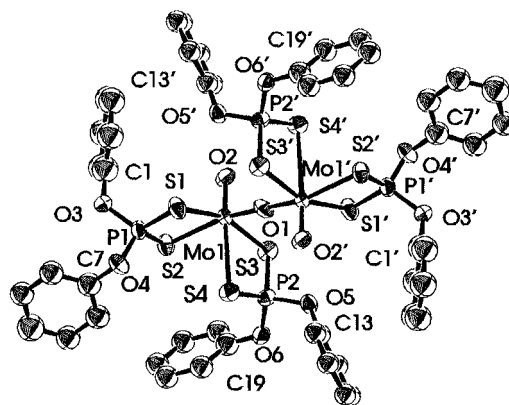
Figure 3. ORTEP plot of the molecule Mo$_2$O$_3$[S$_2$P(OPh)$_2$]$_4$ (**8**). the atoms are drawn with 30% probability ellipsoids. Hydrogen atoms are omitted for clarity.

of the disordered OEt groups omitted for clarity, shows the five-coordination, not including the Mo−Mo interaction, about each of the Mo atoms that is typical of a variety of related Mo$_2$O$_2$-(μ-S)$_2$ L$_2$ species with different ligands including L = [S$_2$-CNH$_2$],[44] [S$_2$(S$_2$C$_2$(CN)$_2$)$_2$],[45] and [S$_2$P{O(*i*-Pr)}$_2$].[29] The coordination around molybdenum can be described as square pyramidal, with the axial Mo−O bonds *cis* to the two bridging sulfur atoms, and in the *syn* configuration. Alternatively, molybdenum may be described as being in tetragonal pyramids because the Mo atoms are situated 0.685 Å above the approximate square planes (mean deviation from plane is 0.162 Å) formed by the bridging and dithiophosphate sulfur atoms attached to molybdenum. The basal planes are tipped away from each other with a dihedral angle of 153.5°. The amount the molybdenum atoms are above the basal plane can also be considered in terms of the extent to which the angles involving the oxygen atom are greater than 90°. Thus the O−Mo−S(bridge) angles are 106.0(4) and 110.8(4)° and the O−Mo−S(ligand) angles are 99.4(4) and 110.8(4)°. These values, as well as the Mo−O distance of 1.66(1) Å, are similar to those reported for Mo$_2$O$_2$(μ-S)$_2$[S$_2${O(*i*-Pr)}$_2$]$_2$,[29] Mo$_2$O$_2$(μ-S)$_2$[S$_2$-CNH$_2$]$_2$,[44] and Mo$_2$O$_2$(μ-S)$_2$-[S$_2$(S$_2$C$_2$(CN)$_2$)$_2$]$_2$.[45] The S−Mo−S ligand bite angle of 78.2(1)° in **1** is similar to those in Mo$_2$O$_2$-(μ-O,S)[S$_2${O(*i*-Pr)}$_2$]$_2$,[28] and, as is to be expected, is larger than those of the dithiocarbamate or 1,1-dicyanoethylene-2,2-dithiolate ligands, which were reported as being close to 71.0°. The Mo$_2$S$_2$ bridging unit is not planar, and the dihedral or fold angle between the two MoS$_2$ planes is 149.3(2)° in **1**, 144.8° in Mo$_2$O$_2$-(μ-S)$_2$[S$_2${O(*i*-Pr)}$_2$]$_2$,[29] and 146.8° in Mo$_2$O$_2$(μ-O,S)[S$_2${O(*i*-Pr)}$_2$]$_2$,[28] so there is a larger change on substituting *i*-Pr for Et in the ligand than in replacing an S atom in the bridge with an O atom. The average Mo−S(bridge) distance of 2.30(2) Å in **1** is the same as in Mo$_2$O$_2$(μ-S)$_2$[S$_2${O(*i*-Pr)}$_2$]$_2$[29] and slightly shorter than in Mo$_2$O$_2$(μ-O,S)[S$_2${O(*i*-Pr)}$_2$]$_2$.[28] The Mo−S(ligand) distances for the essentially bidentate dithiophosphate groups are slightly longer, averaging 2.49(3) Å in **1**. The Mo−Mo distance of 2.823(3) Å in **1** is the same as those reported for Mo$_2$O$_2$(μ-S)$_2$[S$_2$CNH$_2$]$_2$, 2.820(1) Å, Mo$_2$O$_2$(μ-S)$_2$[S$_2$($_2$C$_2$-(CN)$_2$)$_2$], 2.821(2) Å, and even Mo$_2$S$_2$(μ-S)$_2$[S$_2${O(*i*-Pr)}$_2$]$_2$, 2.828 Å.[46] Thus the environment about the molybdenum atoms

(42) Drew, M. G. B.; Baricalli, P. J.; Mitchell, P. C. H.; Read, A. R. *J. Chem. Soc. Dalton Trans.* **1983**, 649.
(43) Baricalli, P. J.; Drew, M. G. B.; Mitchell, P. C. H. *Acta Crystallogr.* **1983**, C39, 843.
(44) Howlader, N. C.; Haight, G. P. Jr.; Hambley, T. W.; Snow, M. R.; Lawrance, G. A. *Inorg. Chem.* **1984**, 23, 1811.
(45) Gelder, J. I.; Enemark, J. H. *Inorg. Chem.* **1976**, 8, 1839.
(46) Huang, J.; Shang, M.; Huang, J.; Zhuang, H.; Lu, S.; Lu, J. *Jiegou Huaxue* **1982**, 1, 1.

is relatively unchanged regardless of the nature of the alkyl group on the phosphate or indeed the nature of the dithio ligand or the presence of Mo−S terminal rather than Mo−O bonds.

The vacant site in the core, which is *trans* to each terminal oxo group, can be occupied to give six-coordinate molybdenum sites, if the Mo−Mo interaction is ignored. Compounds **1** and **4** both give the expected 1:2 pyridine adducts, **6** and **7**, but they differ somewhat in their spectroscopic properties as will be discussed later. Unfortunately, only for $Mo_2O_2(\mu\text{-}S)_2[S_2P\text{-}(OEt)_2]_2\cdot2NC_5H_5$ (**6**) was it possible to grow X-ray quality crystals. The ORTEP diagram of **6** (Figure 2) shows that the positions *trans* to the Mo−O bonds are occupied by pyridine molecules. The average O−Mo−N angle is 169.3(3)° and, although the Mo−N distances of 2.569(7) and 2.545(7) Å are long, they are similar to the two Mo−N distances reported for the mixed bridge species $Mo_2O_2(\mu\text{-}O,S)[S_2P(O(i\text{-}Pr)_2]_2\cdot2$pyridazine.[42] Interestingly, in contrast to **6**, only a 1:1 adduct is formed between $Mo_2O_2(\mu\text{-}O,S)[S_2P(O(i\text{-}Pr)_2]_2$ and pyridine which bridges both molybdenum atoms at distances of 2.97(2) and 2.93(1) Å.[42] Despite the long distance, minor structural differences have been noted, for example in the dihedral angle of the MoOSMo bridges, when the structure of $Mo_2O_2(\mu\text{-}O,S)\text{-}[S_2P(O(i\text{-}Pr)_2]_2$ is compared with that of the crevice compound $Mo_2O_2(\mu\text{-}O,S)[S_2P(O(i\text{-}Pr)_2]_2\cdot NC_5H_5$.[43]

At first sight, the basic core of **1** is virtually unaltered on the introduction of the pyridine molecules to form $Mo_2O_2(\mu\text{-}S)_2\text{-}[S_2P(OEt)_2]_2\cdot2NC_5H_5$ (**6**). The Mo−Mo distance of 2.819(1) Å in **6** is essentially the same as in **1**, as are the S−Mo−S ligand bite angles and the Mo−O bond lengths, while the Mo−S distances, both ligand and bridge, are only slightly longer in **6**. The dihedral angle between the two MoSMo planes of the Mo_2S_2 bridging unit of 151.1(2)° in **6** remains much the same as in **1**. A comparison of the appropriate bond lengths and angles shows that the dimensions within all of the $S_2P(OEt)_2$ ligands in **1** and **6** are essentially the same. However, a notable change occurs in the dihedral angle between the two planes forming the bases of the square pyramids about each molybdenum atom from 153.5° in **1** to 179.1° in **6**. In other words the six sulfur atoms become essentially coplanar (mean deviation from plane is only 0.023 Å) as a result of pyridine filling the vacant coordination site, with Mo(1) and Mo(2) now at 0.366 and 0.357 Å, respectively, above the plane. The O−Mo−S(bridge) angles in **6** average 102.3(4)° compared to 106.0(4) and 110.8(4)° in **1**, and the O−Mo−S(ligand) angles are even closer to 90° in **6**, at an average of 93.4(9)°.

(μ-Oxo)bis[oxobis(*O,O*-diphenyl dithiophosphato)molybdenum(V), $Mo_2O_3[S_2P(OPh)_2]_4$ (**8**), crystallizes in the space group $P2_1/n$. The structures of two analogous alkyl dithiophosphate derivatives have been reported, $Mo_2O_3[S_2P(OEt)_2]_4\cdot2C_6H_4Cl$, for which an *R* value of only 0.117 was achieved,[17] and $Mo_2O_3\text{-}[S_2P(O\{n\text{-}Pr\})_2]_4$, which crystallizes as triclinic in the space group $P\bar{1}$.[47] In general related structures involving aryl substitution in the dithiophosphates, -carbonates, and -carbamates are relatively rare. The bond lengths and bond angles of **8** are displayed together in Table 7. The ORTEP diagram (Figure 3) shows the linear Mo−O−Mo bridge in which, as in related dithiocarbonate[13] and dithiocarbamate[10] derivatives, the Mo−O(bridge) bonds are much longer, 1.8567(1) Å, than the Mo−O(terminal) bonds, 1.66(1) Å consistent with the latter having considerable π-bond character. The two bond distances are not statistically different in $Mo_2O_3[S_2P(O\{n\text{-}Pr\})_2]_4$,[47] $Mo_2O_3[S_2COEt]_4$,[13] or $Mo_2O_3[S_2CN(n\text{-}Pr)_2]_4$.[10] The immediate environment about the molybdenum atoms in all four molecules

is that of a distorted octahedron, with the terminal Mo−O bonds mutually in the **syn** conformation and **cis** to the Mo−O bonds of the linear bridge. One of the dithiophosphate ligands in **8** is bidentate, with an average Mo−S distance of 2.51(5) Å, which is the same as in $Mo_2O_3[S_2P(O\{n\text{-}Pr\})_2]_4$, 2.49(6) Å, $Mo_2O_3[S_2\text{-}COEt]_4$, 2.50(4) Å, and $Mo_2O_3[S_2CN(n\text{-}Pr)_2]_4$, 2.48(4) Å. In the second ligand, the Mo−S bond in the position *trans* to Mo−O(terminal) is considerably longer than all of the other Mo−S bonds in the molecule, while the second Mo−S bond is similar, 2.503(5) Å in **8** and 2.501(2), 2.509(2), and 2.491(5) Å in $Mo_2O_3[S_2P(O\{n\text{-}Pr\})_2]_4$, $Mo_2O_3[S_2COEt]_4$, and $Mo_2O_3[S_2CN(n\text{-}Pr)_2]_4$, respectively, to those of the bidentate ligand. Thus, despite the fact that the bite angle for a bidentate ligand is much smaller (70−71°) in dithiocarbonates and -carbamates than in dithiophosphates (78−80° in **1**, **6** and **8**), the lengths of all the "normal" Mo−S bonds are similar, as are the bond angles involving them or the three Mo−O bonds. The longer Mo−S bond is the exception indicating that any adjustments around Mo in all of these Mo_2O_3[dithio]₄ species involve this weaker interaction. The bond length of 2.831(4) Å in **8** is similar to that in $Mo_2O_3[S_2P(O\{n\text{-}Pr\})_2]_4$, 2.809(3) Å, but significantly longer than in $Mo_2O_3[S_2COEt]_4$, 2.70(2) Å, and $Mo_2O_3[S_2CN(n\text{-}Pr)_2]_4$, 2.68(1) Å, with bite angles of 75.2(1)° in **8** compared to 67.5(2)° in both $Mo_2O_3[S_2COEt]_4$ and $Mo_2O_3[S_2CN(n\text{-}Pr)_2]_4$. The S−Mo−O(terminal) angles are much closer to 180° in the dithiophosphates, 167.5(4) in **8**, compared to 159(2)° in $Mo_2O_3[S_2COEt]_4$ and $Mo_2O_3[S_2CN(n\text{-}Pr)_2]_4$. Although the P−S bond attached to the longer Mo−S bond is the shortest in **1**, **6**, and **8**, it is only slightly shorter, suggesting that there is still an interaction with molybdenum and the bond lengths and angles within all ligands are essentially the same for all three molecules. The similarity of the features in **8** and those reported for the alkyl analogues[17,47] indicates that even the packing effects of eight phenoxy groups replacing eight alkoxy groups are apparently the same at least in terms of the environment about molybdenum.

Vibrational Spectra. Characteristic features of the infrared (mainly) and Raman spectra of compounds **1−7** are given in Table 8. The assignments are based on comparisons with the spectra of the corresponding dialkyl and alkylene dithiophosphoric acids and their salts, as well as reported assignments for various metal dialkyl and alkylene dithiophosphates[42,48] and related oxomolybdenum(V) complexes of *O*-alkyl dithiocarbonate, *O,O*-dialkyldithiocarbamate, and cysteine complexes.[14,44,49] The bands of strong intensity in the infrared spectra associated with the dithiophosphate groups remain largely unchanged in the molybdenum complexes relative to the free acids or their salts. This is not surprising in the light of the similarity of the bond lengths and angles within the dithiophosphate ligands in **1**, **6**, and **8**. The bands include those that have been attributed to ν(PO−C) and ν(P−OC) in the regions 990 to 1045 cm⁻¹ and 766 to 844 cm⁻¹, respectively, and those assignable to ν-(P−S)asym or ν(P=S) and ν(P−S)sym or ν(P−S), which generally appear in the regions 630−680 and 535−580 cm⁻¹, respectively. When compared to the assignments in the parent acids, there is a very small but notable shift ($\Delta\nu = 20-10$ cm⁻¹) to lower frequencies of ν(P=S) in the molybdenum complexes, which is at least consistent with the bidentate nature of the bonding of the ligand to the metal atom.[42]

In general, for two Mo=O bonds in the *syn* conformation with mutually *cis* geometry, as in **1−7**, two bands are expected around 950 cm⁻¹ attributable to asymmetric and symmetric

(47) Ratnani, R.; Bohra, R.; Srivistava, G.; Mehrotra, R. C. *J. Crystallogr. Spectrosc. Res.* **1990**, *20*, 541.

(48) Yader, J. S.; Mehrotra, R. K.; Srivastana, G. *Polyhedron* **1987**, *6*, 1687.
(49) Ueyama, N.; Nakata, M.; Araki, T.; Nakamura, A.; Yamashita, S.; Yamashita, T. *Inorg. Chem.* **1981**, *20*, 1934.

Table 8. Selected Features and Their Assignments in the Vibrational Spectra (cm^{-1}) of Compounds (**1**–**7**)^{a,b}

no.	compd	ν(PO—C)	ν(Mo=O)$_{asym}$	ν(Mo=O)$_{sym}{}^c$	ν(P—OC)	ν(P—S)$_{asym}$	ν(P—S)$_{sym}$	ν(MoS$_2$Mo)$_{asym}$	ν(MoS$_2$Mo)$_{sym}{}^d$	ν(Mo—SL)$_{asym}{}^e$	ν(Mo—SL)$_{sym}{}^e$
1	Mo$_2$O$_2$S$_2$[S$_2$P(OEt)$_2$]$_2$	1040 sh	1004 s,br	968 s	794 ms	639 m	538 m	470 w	441 vw	332 m	270 mw
2	Mo$_2$O$_2$S$_2$[S$_2$P(O{n-Pr})$_2$]$_2$	[990 s,br]^f	990 s,br	966 w	810 m	640 s	564 s	469 w	420 vw	334 m	270 m
3	Mo$_2$O$_2$S$_2$[S$_2$P(O{n-Pr})$_2$]$_2$	[997 s,br]^f	997 s,br	970 sh	766 ms	640 ms	551 ms	461 mw	406 w	336 m	266 w
4	Mo$_2$O$_2$S$_2$[S$_2$POCH$_2$CMe$_2$CH$_2$O]$_2{}^g$	1048 s	979 s	960 sh	824 s	666 m	547 w	461 w	421 w	337 ms	273 w
5	Mo$_2$O$_2$S$_2$[S$_2$POCMe$_2$CMe$_2$O]$_2{}^g$	1015 s	975 s	935 m	815 s	640 s	580 m	480 m	420 w	330 m	270 w
6	Mo$_2$O$_2$S$_2$[S$_2$P(OEt)$_2$]$_2$·2NC$_5$H$_5$	1035 sh	970 s	950 sh	793 ms	[690 s,br]^h	537 m	482 mw	420 w	295 m	260 mw
7	Mo$_2$O$_2$S$_2$[S$_2$POCH$_2$CMe$_2$CH$_2$O]$_2$·2NC$_5$H$_5$	1043 s	963 s	940 sh	820 m	[693 s,br]^h	543 w	451 w,br	420 sh	330 mw	270 w

^{a} Run as KBr pellets to 400 cm^{-1} and as Nujol mulls below 450 cm^{-1}. ^{b} Key: s = strong, m = medium, w = weak, v = very, sh = shoulder, br = broad. ^{c} This is the most intense peak in the Raman effect and is seen at 945, 968, 965, 943 and 965 cm^{-1} in **1**, **3**, **4**, **6** and **7**, respectively. ^{d} This is usually the second most intense peak in the Raman effect and is seen at 425 [40], 428 [50], 420 [25], 421 [60] and 422 [30] in **1**, **3**, **4**, **6** and **7**, respectively. ^{e} L = Ligand. ^{f} The PO—C stretch is expected at approximately 1020 cm^{-1} and is presumably masked by the strong Mo=O asymmetric stretch. ^{g} The ring vibrations occur in this region, at approximately 995 cm^{-1} in **4** and **7**, and 920 cm^{-1} in **5**. ^{h} The asymmetric P—S stretch (or P=S stretch) is obscured by the broad band arising from the presence of the pyridine molecules.

stretches. ν(Mo=O)$_{asym}$ is typically strong in the infrared spectrum, where it occurs in the same region as ring vibrations of alkylene dithiophosphates and as PO=C stretches, particularly in alkyl dithiophosphates. In a relatively rare use of Raman spectroscopy in this field, ν(Mo=O)$_{sym}$ has been unequivocally identified as one of two dominant peaks in the Raman spectrum of Na$_2$[Mo$_2$O$_2$(μ-S)$_2$(cys)$_2$]·4H$_2$O where it is seen at 935 cm^{-1}, along with a peak at 418 cm^{-1}, attributable to the symmetrical bridge stretching mode, ν(MoS$_2$Mo)$_{sym}$.[49] The same phenomenon is noted in the Raman spectra of compounds **1**, **3**, **4**, **6**, and **7**, confirming the corresponding assignments in **1**–**7**. The remaining band in the mid-IR region, which is not seen in the free acids or the salts of the ligands, is around 450–485 cm^{-1} and is assignable to ν(MoS$_2$Mo)$_{asym}$. In the far-IR spectra, bands at approximately 330 and 260 cm^{-1} are assigned to the asymmetric and symmetric stretches involving the Mo—S(ligand) bonds.

The relevant assignments are similar for all compounds and particularly so for the pairings of compounds **1** and **4** with their pyridine adducts, **6** and **7**, consistent with the bond lengths and angles being largely unchanged by the formation of the adducts. The same phenomenon was noted in the vibrational spectra of Mo$_2$O$_2$(μ-O,S)[S$_2$P(O{i-Pr})$_2$]$_2$ and its related pyridine and pyridazine adducts, which also have very long Mo—N bonds that apparently had so little effect on the structures that they were described as "crevice coordination" compounds.[42]

^{1}H NMR Spectra. The crystal structures of Mo$_2$O$_2$S$_2$[S$_2$P(OEt)$_2$]$_2$ (**1**) and its pyridine adduct, Mo$_2$O$_2$S$_2$[S$_2$P(OEt)$_2$]$_2$·2NC$_5$H$_5$ (**6**), demonstrate clearly that the two alkoxy groups attached to phosphorus are *syn* and *anti* relative to the M=O bond. The ^{1}H NMR spectral data, which are summarized in Table 9 for compounds **1**–**7**, demonstrate that this situation is maintained in solution, not only for **1** and **6**, but also for the alkoxy groups in **2** and **3** as well as the glycoxy groups in **4**, **5**, and **7**. The non-equivalence of the groups attached to phosphorus is the primary feature of the ^{1}H (and ^{13}C) NMR spectra and all of the bis(μ-sulfido)bis[{*O*,*O*-dialkyl (alkylene) dithiophosphato}oxomolybdenum(V)] compounds (**1**–**5**) as well as the pyridine adducts (**6**, **7**) have splitting patterns and relative intensities that are consistent with the solid state structures being maintained in solution. Thus, for example, the ethyl groups in Mo$_2$O$_2$S$_2$[S$_2$P(OEt)$_2$]$_2$ (**1**) are essentially identifiable in terms of first-order spectra with the CH$_2$ groups seen as two sets of doublets of quartets and the CH$_3$ groups as two sets of triplets. The two sets arise from the non-equivalence of the OEt groups, and the values of the J(PH) and J(HH) coupling constants giving rise to the doublet of quartets are of the expected magnitude. The multiplet observed for the protons on the central atom in the OCH$_2$CH$_2$CH$_3$ groups in Mo$_2$O$_2$S$_2$[S$_2$P{O(n-Pr)}$_2$]$_2$ are as predicted for both J(HH) coupling constants having the same value, and the nine-line multiplet for the OCH groups in Mo$_2$O$_2$S$_2$[S$_2$P{O(i-Pr)}$_2$]$_2$ arises from the fact that fortuitously the value of J(PH) is twice that of J(HH). In general, papers involving the related dithiocarbamates have made no mention of similar nonequivalence. The presence of the pyridine molecules is clearly seen in the NMR spectra of **6** and **7**. The splitting patterns and chemical shifts of the ethoxy groups in **1** and **6** are virtually the same, consistent with the similarities in the solid state structures of **1** and **6**. The weakness, and possibly orientation, of the Mo—N coordinate bond presumably accounts for the fact that the chemical shifts attributable to the pyridine molecules are very close to those of pyridine itself. By contrast, the chemical shifts of the pyridine molecules in Mo$_2$O$_2$S$_2$-[S$_2$POCH$_2$CMe$_2$CH$_2$O]$_2$·2NC$_5$H$_5$, **7**, are different from those of free pyridine, possibly indicating a difference in the nature of

Table 9. ^{1}H NMR Chemical Shifts for the Bis(μ-sulfido)bis[{*O,O*-dialkyl (alkylene) dithiophosphato}oxomolybdenum(V) Compounds **1**−**7**$^{a-c}$

no.	compd	O−CH₂	OC−CH₃/−CCH$_n$	OCCCH₃
1	Mo₂O₂S₂[S₂P(OEt)₂]₂	3.90 (4H, dq, *J*(PH) = 9.7; *J* = 7.0)	1.29 (6H , t, *J* = 7.0)	
		4.65 (4H, dq, *J*(PH) = 9.5; *J* = 7.0)	1.57 (6H, t, *J* = 7.0)	
2	Mo₂O₂S₂[S₂P{O(*n*-Pr)}₂]₂	3.86 (4H, dt, *J*(PH) = 9.6; *J* = 7.0)	1.59 (4H, m, *J* = 7.0)^d	0.93 (6H, t, *J* = 7.0)
		4.59 (4H, m, *J*(PH) = 9.6; *J* = 7.6)	1.93 (4H, m, *J* = 7.0)d	1.11 (6H, t, *J* = 7.0)
3	Mo₂O₂S₂[S₂P{O(*i*-Pr)}₂]₂	4.33 (2H, m, *J*(PH) = 12.2; *J* = 6.1)^e	1.28 (12H, d, *J* = 6.1)	
		5.31 (2H, m, *J*(PH) = 12.2; *J* = 6.1)^e	1.58 (12H, d, *J* = 6.1)	
4	Mo₂O₂S₂[S₂POCH₂CMe₂CH₂O]₂	4.18 (4H, d, *J*(PH) = 15.1)	1.20 (6H, s)	
		4.37 (4H, d, *J*(PH) = 15.0)	1.21 (6H, s)	
5	Mo₂O₂S₂[S₂POCMe₂CMe₂O]₂		1.19 (6H, s)	
			0.85 (6H, s)	
6	Mo₂O₂S₂[S₂P(OEt)₂]₂·2NC₅H₅^f	3.88 (4H, dq, *J*(PH) = 9.7; *J* = 7.0)	1.28 (6H, t, *J* = 7.0)	
		4.64 (4H, dq, *J*(PH) = 9.6; *J* = 7.0)	1.56 (6H, t, J = 7.0)	
7	Mo₂O₂S₂[S₂POCH₂CMe₂CH₂O]₂·2NC₅H₅^g	4.03 (8H, d, *J*(PH) = 15.6)	1.03 (12H, s)	

^{a} The spectra were recorded in CDCl₃ and reported in ppm from Me₄Si. ^{b} Number of protons and multiplicities are in parentheses (s = singlet; d = doublet, t = triplet; q =quartet; m = multiplet). ^{c} Coupling constants in Hz indicated by *J*(PH) and *J* for PH and HH coupling, respectively. ^{d} Both *J*(HH) coupling constants have the value 7.0 Hz. ^{e} Multiplet arises from the exact overlap of a doublet of septets to give a nine line 1:6: 16:26:30:26:16:6:1 multiplet. ^{f} Peaks arising from NC₅H₅ are seen centered at 8.58 (4 H), 7.66 (2 H) and 7.29 (4 H) ppm. ^{g} Peaks arising from NC₅H₅ are seen centered at 8.90 (4 H), 8.12 (2 H) and 7.66 (4 H) ppm.

Table 10. ^{13}C and ^{31}P NMR Chemical Shifts for the Bis(μ-sulfido)bis[{*O,O*-dialkyl (alkylene) dithiophosphato}oxomolybdenum(V)] Compounds **1**−**7**^{a,b}

no.	compd	O−CH₂	OC−CH₃/−CCH$_n$	OCCCH₃	^{31}P
1	Mo₂O₂S₂[S₂P(OEt)₂]₂	67.20 (d, *J*(PC) = 3.6)	16.08 (d, *J*(PC) = 7.4)		111.9
		65.56 (br)^c	15.78 (d, *J*(PC) = 7.3)		
2	Mo₂O₂S₂[S₂P{O(*n*-Pr)}₂]₂	70.04 (d, *J*(PC) = 4.9)	23.18 (d, *J*(PC) = 7.3)	10.13 s	111.1
		71.94 (d, *J*(PC) = 4.9)			
3	Mo₂O₂S₂[S₂P{O(*i*-Pr)}₂]₂	75.51 (d, *J*(PC) = 5.2, 7.3)	23.88 (d, *J*(PC) = 3.7, 4.9)		107.8
		77.68 (d, *J*(PC) = 5.0, 6.1)	23.71 (br)^c		
4	Mo₂O₂S₂[S₂POCH₂CMe₂CH₂O]₂^d	77.80	32.87	21.70	108.0
5	Mo₂O₂S₂[S₂POCMe₂CMe₂O]₂	93.02	24.08 (d, *J*(PC) = 3.67)		124.0
6	Mo₂O₂S₂[S₂P(OEt)₂]₂.2NC₅H₅^e	67.16 (d, *J*(PC) = 4.3)	16.07 (d, *J*(PC) = 7.7, 7.0)		112.2
		65.49 (d, *J*(PC) = 4.8)	15.76 (d, *J*(PC) = 8.4, 7.0)		
7	Mo₂O₂S₂[S₂POCH₂CMe₂CH₂O]₂·2NC₅H₅^f	75.15 (d, *J*(PC) = 7.6)	32.68	21.99	109.0

^{a} The spectra were recorded in CDCl₃ and reported in ppm from Me₄Si for ^{13}C and from H₃PO₄ for ^{31}P. ^{b} d = doublet; values of *J*(PC) coupling constants in Hz. ^{c} Value of *J*(PC) presumably too small to be clearly identified. ^{d} Not very soluble. ^{e} Peaks arising from NC₅H₅ are seen at 149.55, 136.22 and 123.78 ppm. ^{f} Peaks arising from NC₅H₅ are seen at 145.12, 141.65 and 125.60 ppm.

the coordination from that in **6**. Further, in contrast to the situation for **1** and **6**, the ^{1}H NMR spectrum of **7** also differs from that of **4** in that the chemical shifts are not as similar and only single peaks are seen. This suggests strongly that the structure of **7** differs from that of **6** although the relative lack of solubility of itself may be part of the problem, and unfortunately, we were not able to grow suitable crystals of **7** for X-ray studies.

^{13}C NMR Spectra. The ^{13}C NMR spectral data for compounds **1**−**7** are displayed in Table 10. The data for **1**−**3** and **6** also indicate the nonequivalence of the two alkoxy groups attached to phosphorus and show the expected two separate signals for the carbon atoms. The chemical shifts and values of the coupling constants are typical for a variety of dithiophosphate compounds, and once again, the chemical shifts of the peaks attributable to the weakly-bonded pyridine in Mo₂O₂S₂-[S₂P(OEt)₂]₂·2NC₅H₅, **6**, are similar to those of free pyridine. The data for the much less soluble compounds, **4**, **5**, and **7**, are ill-defined by comparison, so it is speculative to suggest that the relatively broad peaks arise from overlap of slightly separated signals, which are each further split slightly by P−C coupling. The chemical shifts of peaks attributable to pyridine in **7** differ from those of free pyridine, again suggesting that the coordination in **7** differs from that in **6**.

^{31}P NMR Spectra. The ^{31}P NMR spectra data of compounds **1**−**7** are also displayed in Table 10. A relatively sharp, singlet is seen in all compounds, indicating that only one phosphorus-containing compound is present in each case in solution and that the phosphorus nuclei are equivalent. The ^{31}P NMR chemical shifts for these derivatives are approximately 26.0−32.0 ppm downfield from those of the parent dithiophosphoric acids. This is to be expected because such downfield shifts are claimed to be indicative of the presence of strong bidentate ligands.[50]

(50) Glidewell, C. *Inorg. Chim. Acta* **1977**, 159.